INVESTIGATING WIND CATCHERS AND SOLAR CHIMNEYS TO IMPROVE THERMAL COMFORT FOR MULTI-UNIT RESIDENTIAL BUILDINGS IN INDIA

Wei-Chih Huang, Marianne Touchie

ABSTRACT

Controlling interior temperatures in buildings is energy intensive, particularly in extreme climates. The increasing demand for cooling in developing countries, driven by a growing middle class, threatens to pose a significant burden on the electricity grid. This increasing energy use along with the pressure to reduce greenhouse gas emissions has led to the exploration of passive cooling technologies. The Initiative for Global Urban Shelter at the University of Toronto's Centre for Global Engineering has been exploring methods to implement passive cooling strategies in Mumbai's new high-rise residential developments for the Slum Rehabilitation Authority (SRA). This exploratory study integrates solar chimneys and wind catchers in a single-loaded corridor configuration. Previous studies have analyzed these solutions independently but their synergistic benefits have not been well documented in multi-unit residential buildings. The effectiveness of the cooling technologies was assessed through spreadsheet calculations. By applying these natural ventilation approaches together in a building form that allows for cross-ventilation, the total number of hours where thermal comfort needs are satisfied exceeds either solution on its own. The combined solution is estimated to reduce thermal discomfort time by a minimum of 81% throughout a typical meteorological year (TMY2). These preliminary findings will be used conduct a more detailed analysis using computational fluid dynamics (CFD) to determine the resultant air velocity for occupants in the suite. The findings of this study will be used to influence the SRA building design to promote a sustainable approach to providing thermal comfort in these new high-rise multi-family developments.

INTRODUCTION

India has undergone drastic changes in both its economic growth and rate of urbanization during the latter half of the past century. This has led to rapid city development and high urbanization rates without adequate infrastructure and proper urban planning to support the growth. Thus, large slum neighborhoods have been established throughout the country's urban centers. The government is improving the standard of living for its slum-dwelling population by transitioning them to formal housing in multi-unit residential buildings (MURBs). However, the energy demands associated the shift to higher living standards must be considered to meet the country's energy reduction targets; a 33-35% reduction in greenhouse gas emissions per GDP in 2030 compared to baseline levels (The World Bank, 2016).

The Slum Rehabilitation Authority of India (SRA) has introduced "The Slum Rehabilitation Redevelopment Project": an initiative to relocate slum inhabitants into formal housing. The goal is to provide current slum

dwellers with land security, appropriate shelter, and access to basic services through the development of new MURBs. The University of Toronto has partnered with the SRA through the Initiative of Global Urban Strategies to develop best practices to help guide the development of the new infrastructure with regards to safety and sustainability.

At this early stage in the slum rehabilitation, there is an opportunity to address energy concerns by altering the built form to incorporate passive cooling solutions. This paper describes an alternative design in which wind catchers and solar chimneys are used to promote passive cooling and increase thermal comfort in comparison to the currently proposed conventional MURB design. Although the solution is designed for Mumbai, the methodology can be adapted to determine the feasibility of a wind catcher and solar chimney solution in different environments, including North America where cooling loads are on the rise.

Climate and Weather

Mumbai is a coastal city located in a tropical climate with annual solar intensity averages of 4.5 to 5.0 kWh/m^2/day (48-54 kWh/ft^2/day) (Ministry of New and Renewable Energy, n.d.). The Indian Meteorological Department defines four climatological seasons: winter (January-February), pre-monsoon (March-May), southwest monsoon (June-September), and post-monsoon (October-December)(India Meteorological Department, n.d.). From the typical meteorological year data provided by ISHRAE (2005), monsoon seasons are dominated by strong westerly winds whereas the winter seasons are dominated by weak northerly winds as illustrated by the seasonal wind roses in Figure 1. The strong winds during the peak cooling periods provide a promising basis for the implementation of a wind catcher.

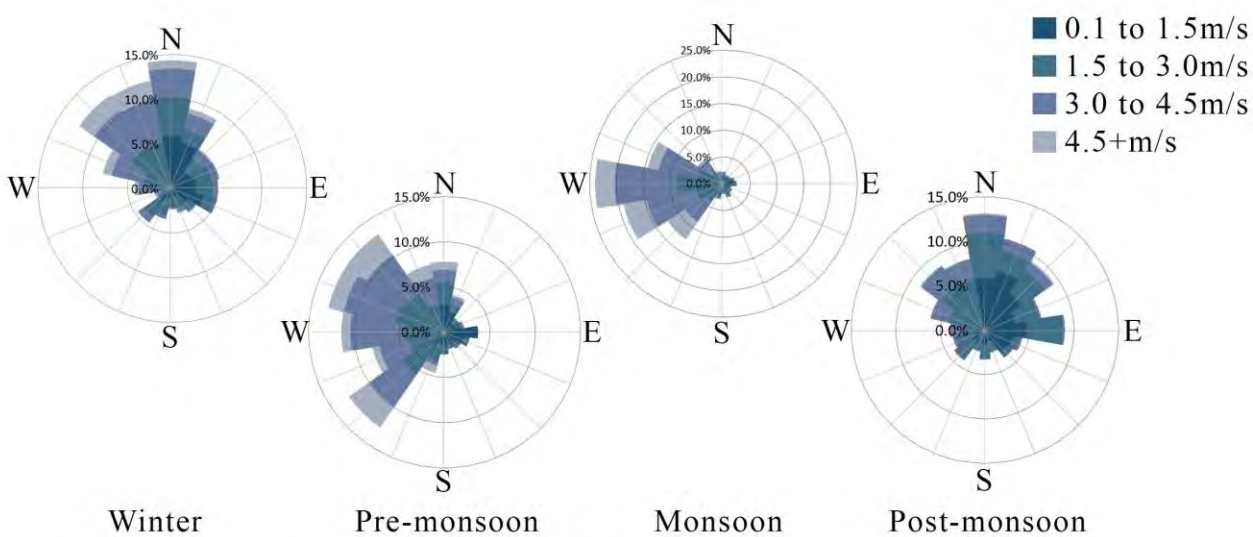

Figure 1: Seasonal wind roses for Mumbai based on TMY2 weather data from ISHRAE (2005)

Cooling Energy Demand and Affordability

Passive cooling strategies may be a viable low-cost and low-energy alternative to active cooling strategies, particularly for very low-income households. Passive cooling technologies can reduce latent and/or sensible heat energy within the building envelope without the consumption of electricity. These approaches could present a method to achieve thermal comfort for residents transitioning from slums to formal housing in

MURBs.

Given the high annual temperatures, space cooling is required for occupants to be thermally comfortable. India's Bureau of Energy Efficiency estimates that fans, air coolers and air conditioners consume 34%, 7% and 7%, respectively, of the total energy demand of residential buildings (Indraganti, 2010a). Table 1 summarizes the number and energy consumption characteristics of residential cooling appliance use in India in 2006 and their projected values in 2031.

Table 1: Residential cooling appliance use and annual cooling energy demand in India (The World Bank, 2008).

		Fans	*Air Cooler*	*Air Conditioner*
2006	Number of Units in India (M)	228.9	22.5	2
	Average Power Consumption (W)	39	250	1,973
	Annual Operation Time (hr/year) (%)	2,520 (28.8)	1,440 (16.4)	575 (6.5)
	Annual Energy Demand (GWh)	22,496	8,100	2,269
2031 Projections	Number of Units in India (M)	1,091.7	168.9	48
	Average Power Consumption (W)	36	230	1,809
	Annual Operation Time (hr/year) (%)	2,520 (28.8)	1440 (16.4)	575 (6.5)
	Annual Energy Demand (GWh)	99,039	55,939	49,928

The capital and operating costs of air coolers and air conditioners are unaffordable for the average slum household. It is estimated that approximately 41% of slum households have an average monthly income between ₹5,000 (CAD 97.60) to ₹10,000 (CAD 195.20) (Society for Participatory Research in Asia, 2014). With electricity costs ranging between ₹2.9/kWh (CAD 0.06/kWh) to ₹7.65/kWh (CAD 0.15/kWh)(Bijli Bachao Team, 2017), air conditioning costs would represent 8% to 20% of their current monthly income.

PROPOSED DESIGN ALTERNATIVE

Increasing the air movement within the suites can mitigate the hot thermal discomfort. Increased air movement will increase convective heat losses and latent heat losses when the body is perspiring. Wind catchers and solar chimneys were investigated as options to increase air movement in the proposed design because of their proven effectiveness in previous studies (Fatimah et al., n.d., Carrilho da Graça et al., 2002, Priyadarsini et al., 2004, Li and Li, 2015). The variations in perceived comfort and environmental conditions make it difficult to determine the maximum temperature threshold where the increased air movement would no longer improve thermal comfort. As such, thermal comfort will be defined strictly by the various thermal comfort models described below for the purposes of this exploratory study.

Wind Catcher

Wind catchers have been used in traditional Egyptian and Middle Eastern architecture in various forms (Gallo, 1996). Wind catchers use large "catchers" located at the tops of buildings to capture and redirect wind into the building to promote indoor air movement. Numerous studies have explored the various effects of wind catchers including Mavrogianni and Mumovic (2009), Priyadarsini et al. (2004), and Da Graça et al. (2002). Adaptations of this approach, such as earth tubes, use the Earth's large thermal mass as a heat sink to reduce inlet temperatures. Calautit & Hughes (2014) has explored the impact of outfitting wind catcher inlets with heat sinks. Furthermore, inlet velocities could be assisted by mechanical fans during periods of low winds.

Mumbai's climate is a promising environment for wind catchers given the consistency of the wind direction and high wind speeds during the hottest seasons: the pre-monsoon and monsoon seasons. The proposed design includes wind catchers extending from the top of the building, along the elevation and into each suite. Inlets would be placed above the roof of the building to avoid the turbulent air flow and varying pressure coefficients caused by the faces of the building and the negative pressures at the roof surface.

Solar Chimney

A solar chimney will drive air movement through stack effect when the sun shines regardless of the wind conditions. The chimney consists of an absorber wall against the building exterior with a glass panel in front. The radiation emitted from the absorber wall will heat the air column created by the glass wall and decrease the air density. The hot air will rise out of the chimney and pull cool air from lower openings at each individual suite. For the purposes of the study, the absorber wall is assumed to be a dark material with relatively low heat capacity to maximize temperature gains from the incoming irradiation. It should be noted that larger heat capacities would lengthen the operational time of the chimney but have lower average flow rates. The back of the absorber wall would be insulated to prevent heat from being conducted into the building and to increase the transfer from the absorber wall into the air column. Many studies have demonstrated the feasibility of solar chimneys including Bansal et al. (1993), Lee and Strand (2009) and Amori and Mohammed (2012).

Solar chimneys are effective given that the chimney would be operational when the solar gains and the corresponding cooling demand are at their highest. Positioning the solar chimney on the south-facing wall would maximize the total operating time of the chimney. As Mumbai is relatively close to the Tropic of Cancer (19°N), solar irradiation would strike the north face for some parts of the year. The solar chimney would also be inoperable during overcast periods with low irradiation. As these conditions vary, the solar irradiance from the TMY2 data is assumed to reflect Mumbai's weather patterns.

Benefits of a Combined System

A mock-up of the combined system is shown in Figure 2. Neither the wind catcher nor the solar chimney will operate for all periods when cooling is required because they are powered by naturally varying phenomena. However, the downtime could be reduced through the implementation of both systems. The combined system would be operational during sunny periods with no wind from the solar chimney and vice versa during windy periods and no sunlight from the wind catcher. Furthermore, the addition of the wind catcher could reduce the occurrence of reverse flow in the solar chimney. Several studies regarding solar chimneys have shown that the heated air is occasionally funnelled back into the suites when the buoyancy force is insufficient (Su et al., n.d., Asadi et al., 2016). Reverse flow could be prevented by initializing the solar chimney with air movement in the correct direction provided by the wind catcher.

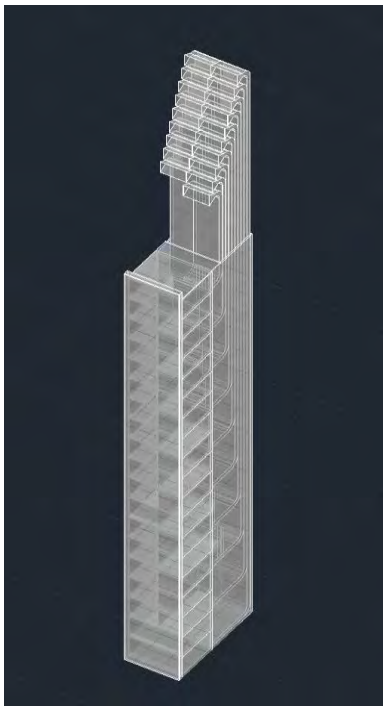

Figure 2: Conceptual drawing of a wind catcher and solar chimney setup for a single column of MURB units.

Under this system, the wind catcher will provide the suite supply air and the solar chimney will generate the negative pressure to drive exhaust from the suite via two separate channels. Zamora & Kaiser (2010) and Nouanégué & Bilgen (2008) have numerically solved for airflow rates where the effects of exterior wind conditions on an operational solar chimney are modeled. In comparison, the proposed solution would build upon their ideas through the addition of separate air channel to redirect air into the MURB suites. Although studies have examined the synergy between the solar chimney and wind catchers within small residential buildings, the implementation of two moving air channels on MURBs and the challenges posed by its magnitude should be explored to promote new passive cooling technologies.

METHODOLOGY

The following section outlines the processes used to evaluate the effectiveness in improving thermal comfort within the suites for the proposed solution. First, using various thermal comfort models, a quantitative analysis of the current state with no cooling technologies was established as the base case using the Typical Meteorological Year (TMY2) data for Mumbai. Next, the air speeds at the suite inlet or supply (wind catcher) and the suite outlet or exhaust (solar chimney) were estimated for the following scenarios: the wind catcher only (Scenario W), solar chimney only (Scenario S), and combined solution (Scenario C). The results were compared to the base case to determine the increase in thermal comfort time for each scenario. Note that the velocities of the windcatcher outlet and solar chimney inlet at the suite level, not on an occupant, were used to determine the impact on the thermal comfort indicators. The preliminary feasibility analysis presented in this paper will be followed by extensive computational fluid dynamics (CFD) modelling to determine the impact of these measures on the occupant directly. This section begins with a description of the various thermal comfort models employed in this analysis. Then, the calculations to support the feasibility assessment of the wind catcher and solar chimney are described.

Thermal Comfort Models

ASHRAE Standard 55 defines thermal comfort as "the condition of mind that expresses satisfaction with the thermal environment" (ASHRAE, 2013). Both physical and psychological factors impact the acceptable range of comfort experienced by a population. As such, the comfort range of one population is not applicable to another. Populations living in hot climates are generally more tolerant of higher temperatures than those living in cold climates. Those exposed to naturally ventilated conditions are also more tolerant to a broader range of temperatures as opposed to those in conditioned environments. It has become increasingly suggested within the literature that the widely-accepted thermal comfort standards proposed by ASHRAE are not universally applicable (Singh et al., 2011)(Indraganti, 2010b).

Several thermal comfort models were considered to determine the effectiveness of the proposed solution. These models are the Predicted Mean Vote index (PMV) and the Predicted Percentage of Dissatisfied (PPD) described in ASHRAE Standard 55, a corrected PMV index (cPMV) created by Singh et al. (2011) and a corresponding corrected PPD (cPPD), and the Tropical Summer Index (TSI) recommended by the National Building Code of India (Udaykumar et al., 2013). ASHRAE Standard 55 was used to establish a universal baseline for comparison whereas the cPMV and TSI models were designed to better reflect the thermal sensations experienced by the local population.

ASHRAE Standard 55 (PMV, PPD)

ASHRAE Standard 55: Thermal Environmental Conditions for Human Occupancy defines the various conditions and procedures required for acceptable thermal environments. The standard uses the PMV model with a 7-point scale where +3 is "hot", -3 is "cold" and 0 is "neutral" (ASHRAE, 2013b). To satisfy the standard, values should be between -0.5 and 0.5 corresponding to a Predicted Percentage Dissatisfied (PPD) of less than 10%. Parameters which influence PMV values include the body surface area, clothing surface area and insulating value, sensible and evaporative heat losses from the skin and the clothing to the environment, metabolic rate, and the radiant heat exchange with the person's surroundings.

Corrected PMV (cPMV)

Singh (2011) proposes the use of a corrected PMV (cPMV) model determined through a survey of North-Eastern Indian residents. Thermal comfort data was collected through questionnaires based on ASHRAE 55-2004 Informative Appendix E and clothing values determined by ISO 7730. The survey included 150 households representing 300 residents. The participants were surveyed throughout the year to capture the effects of the various climatological seasons. Singh could determine an "actual mean vote" which represented the thermal sensation of the residents more accurately than the generic PMV model used in ASHRAE. The correlation between Singh's results and the PMV model are shown in Equation 1 and Equation 2 for summer and winter, respectively (Singh et al., 2011).

$$cPMV = \frac{PMV}{1+0.444\times PMV}\ (Summer - July) \quad (1)$$

$$cPMV = \frac{PMV}{1-0.9\times PMV}\ (Winter - January) \quad (2)$$

The results showed that participants had a greater tolerance range for temperatures in the summertime and the wintertime when compared to PMV. As opposed to a downwards shift from the PMV values, thermal

discomfort during the winter is also lower. It is suspected that the wider range of tolerance from being accustomed to naturally ventilated indoor environments outweighed the respondents' acclimatization to warmer conditions. For reference, a PMV of +1 (26% PPD) during the summer would translate to a cPMV of +0.69 (15% cPPD).

Tropical Summer Index (TSI)

The National Building Code of India recommends use of the Tropical Summer Index to determine thermal comfort (Udaykumar et al., 2013). The formula for TSI is shown in Equation 3 (Udaykumar et al., 2013).

$$TSI = 0.308t_w + t_g - 2.06\sqrt{V + 0.841} \tag{3}$$

Where: t_w is the wet bulb temperature [°C]; t_g is the dry bulb temperature [°C]; V is the air velocity [m/s]; there are no units for the TSI.

TSI values below 19 or exceeding 34 would be equivalent to exceeding the 10% PPD used in ASHRAE where high TSI values represent being "too hot" and low being "too cold" (Udaykumar et al., 2013).

Baseline Thermal Comfort Level

A quantitative assessment of the baseline thermal comfort without the use of cooling technologies was determined through the various thermal comfort models discussed. PMV, cPMV, PPD, cPPD and TSI calculations were performed in Microsoft Excel using TMY2 data from ISHRAE (2005). Several assumptions were made to calculate PMV as described here and summarized in Table 2. First, occupants are assumed to have access to and wear the appropriate clothing to minimize their thermal discomfort with clo values varying between 0.5 clo (typical indoor summer ensemble) to 1 clo (typical indoor winter ensemble). The metabolic rate was set to equal 1.0 met for a seated occupant at rest. External work was set to zero. The surrounding air velocity was assumed to be relatively still at 0.15 m/s (0.5 ft/s) (ASHRAE, 2013). The thermal mass and insulation of the building, which causes the thermal lag between the two environments, is unknown and could not be accounted for in this study. Therefore, it was assumed that the interior temperature and relative humidity were equal to the hourly outdoor dry bulb temperature and relative humidity values from the weather file. Lastly, the mean radiant temperature was assumed to be equal to the current ambient air temperature.

Table 2: Assumptions used to determine PMV values

Variable	Value
Clothing insulation value [clo]	0.5-1.0
Metabolic rate [met]	1.0
External work [met]	0
Air velocity [m/s] (ft/s)	0.15 m/s (0.5 ft/s)
Air temperature [°C]	Hourly exterior dry bulb temperature
Mean radiant temperature [°C]	Hourly exterior dry bulb temperature
Relative humidity [%]	Hourly exterior relative humidity

Wind Catcher Calculations

To assess the feasibility of the wind catcher, it is necessary to determine the outlet velocity at the suite level supply grille. The velocity pressure at the inlet of the wind catcher (outdoor air intake) is reduced by the pressure drop from the ducts and the fittings used to convey the outdoor air to the suite. The pressure losses in the ducts from friction and fittings were calculated using the fundamental equations presented in the Principles of Heating Ventilating and Air Conditioning (Sauer et al., 2013). To minimize pressure drop from the fittings, the wind catcher was designed for a single inlet (conical, converging bellmouth, L/D=1.0, θ=60) and two elbows (90° elbow, r/W≥2.0, H/W=8.0) resulting in a total loss coefficient of 0.4 (Sauer et al., 2013). The resulting outlet velocity of the wind catcher will vary depending on the width and depth of the duct and the associated friction losses. As such, a range of expected velocity pressures at the suite level supply grille were established to determine the associated maximum acceptable friction loss and the physical dimensions of the duct.

To begin, it is assumed that the pressure losses are a function of the outlet velocity pressures such that feasible duct dimensions can be determined. A ratio of outlet velocity pressure to the inlet velocity pressure is used to simplify the calculations and reduce the number of unknown variables, as shown in Equation 4. The resulting duct dimensions are then used for a discretized calculation procedure to determine more accurate outlet to inlet velocity ratios.

$$\frac{p_{v,intlet}}{p_{v,outlet}} = \frac{p_{v,outlet}}{p_{v,outlet}} + \left(f_d\left(\frac{L}{D}\right) + \sum_{i=1}^{n} C_i\right)\frac{p_{v,outlet}}{p_{v,outlet}} \tag{4}$$

Where: $P_{v,outlet}$, $P_{v,\mathrm{in}let}$ is the velocity pressure at the outlet and inlet respectively [Pa]; f_d is the friction factor, L is the length of the duct [m], D is the inside diameter of the duct [m], C_i is the local loss coefficient, i is the numerical counter for each fitting.

The final form of Equation 4 is shown in Equation 5.

$$P_{v,r} = \left(1 + f_d\left(\frac{L}{D}\right) + \sum_{i=1}^{n} C_i\right)^{-1} \tag{5}$$

Where: $P_{v,r}$ is the ratio of outlet velocity pressure to inlet velocity pressure.

From Equation 5, the maximum acceptable friction loss and minimum duct dimensions can be determined if $P_{v,r}$ is specified. $P_{v,r}$ can be converted to a velocity ratio from fundamentals, shown in Equation 6.

$$P_{v,r} = \left(\frac{V_{outlet}}{V_{inlet}}\right)^2 \tag{6}$$

Outlet to inlet velocity ratios were set at intervals between 0 and 1 at increments of 0.1 to determine the minimum required dimensions of the wind catcher ducts to reach certain outlet velocity targets. Table 3 summarizes the duct dimensions required to maintain a certain percentage of the outdoor wind velocity at the suite level supply opening for ground level units.

Table 3: Duct dimensions required to maintain a specific proportion of outdoor air velocity at the suite level.

V_{outlet}/V_{inlet}	**0.7**	**0.6**	**0.5**	**0.4**	**0.3**	**0.2**	**0.1**
Minimum diameter size [m] (ft)	7.77 (25.5)	3.56 (11.7)	2.44 (8.00)	1.94 (6.36)	1.68 (5.51)	1.53 (5.02)	1.45 (4.76)

The duct dimensions generated using the simplified equation are used for discretized calculation. Equation 4 assumes that the losses from the friction and fittings are a function of the outlet pressure. However, the velocity and the corresponding frictional losses decrease as the air travels further into the catcher. Furthermore, the simplified method also ignores the sequencing of the various parts of the catcher. For example, frictional losses due to length would be lower if all three elbows occurred consecutively before the main duct. These issues can be avoided by recalculating a new velocity pressure along each step of the wind catcher inlet to the suite-level outlet. For a calculation using 10,000 length steps, the formula is shown in Equation 7.

$$V_{inlet}{}^2 = V_{outlet}{}^2 + \sum_{i=1}^{n} V_i{}^2 C_i + \sum_{j=1}^{10,000} V_j{}^2 f_d \left(\frac{L}{10,000D}\right) \tag{7}$$

Where: V_{inlet}, V_{outlet} is the velocity at the wind catcher inlet and outlet respectively [m/s]; i is the numerical counter for each fitting within the wind catcher, V_i is the mean velocity across fitting i [m/s], C_i is the local loss coefficient of fitting i, j is the numerical counter for each L/10,000 step, V_j is the initial velocity at distance jL/10,000 [m/s], f_d is the friction factor, L is the length of the duct [m], D is the inside diameter of the duct [m].

The simplified method in Equation 4 provides an initial estimate of duct sizing which can then be used for the discretized equation. A comparison of the outlet to inlet velocity ratio between the two calculation methods is shown in Table 4.

Table 4: Comparison between the outlet to inlet velocity ratio using the simplified and discretized calculation methods for various duct sizes.

Minimum diameter size [m] (ft)	7.77 (25.5)	3.56 (11.7)	2.44 (8.00)	1.94 (6.36)	1.68 (5.51)	1.53 (5.02)	1.45 (4.76)
V_{outlet}/V_{inlet} **(Simplified)**	0.70	0.60	0.50	0.40	0.30	0.20	0.10
V_{outlet}/V_{inlet} **(Discrete)**	0.50	0.42	0.23	0.06	-	-	-

Based on Table 4, it is possible to achieve up to 50% of the outdoor wind speeds at the suite-level outlet. Three scenarios with varying wind velocity ratios were selected for the thermal comfort model calculations to determine the additional increase in thermal comfort time as wind catcher dimensions increase. The ratios used are a 10% (Scenario W10), a 30% (Scenario W30) and a 50% (Scenario W50) of the outdoor air inlet velocities at the suite-level outlet. As an example, Scenario W10 would denote a MURB with only a wind catcher where the pressure losses due to the duct dimensions would result in 10% of the outdoor air inlet velocity remaining at the suite-level. The outdoor air inlet velocities were determined using equations by Aynsley et al. (1977) to adjust the TMY2 wind speeds collected at an airport weather station to account for the added surface roughness in the urban region where these MURBs will be constructed. The minimum height of the wind catcher above the MURB (9.7m) was determined from Wilson (1979). The outlet velocity of the wind catcher will be directly used for the various thermal comfort indicators.

Solar Chimney Calculations

Calculations for the air velocities generated at the suite-level by the solar chimney are iterative and dependent on multiple factors. Each of the three governing equations (Equation 8, 9, 10) are dependent upon one another: the velocity calculation is dependent on the outlet temperature, the outlet temperature is dependent on the air velocity and the convective heat transfer coefficient, and the convective heat transfer coefficient is dependent on the velocity. The air velocity [m/s] in the chimney can be calculated using Equation 8 (Lee and

Strand, 2009).

$$V = C\sqrt{2gh\frac{T_i - T_o}{T_i}(1 + A_r)^{-2}} \tag{8}$$

Where: V is the velocity of the air [m/s], C is the discharge coefficient; g is the gravitational acceleration [m/s^2]; h is the height of the air column [m]; T_I is the inlet air temperature [K]; T_o is the outlet air temperature [K]; A_r is the outlet area to inlet area ratio.

The outlet temperature [K] is calculated using Equation 9 (Lee and Strand, 2009). The equation determines the air temperature along the length of the chimney. One thousand length steps were used in the calculation. The temperature at the last step (T_{1000}) of the solar chimney would correspond to the outlet velocity used in Equation 8.

$$h_{wf}\left(T_w - \frac{T_{n+1}+T_n}{2}\right) + h_{gf}\left(T_g - \frac{T_{n+1}+T_n}{2}\right) = \frac{mC_{p,a}(T_{n+1}-T_n)}{\Delta xw} \tag{9}$$

Where h_{wf} is the convective heat transfer coefficient between the wall and the fluid [W/m^{2}K], h_{gf} is the convective heat transfer coefficient between the glass and the fluid [W/m^{2}K], T_w is the temperature of the wall [K], T_g is the temperature of the glass [K], T_n, T_{n+1} are the air temperatures at various n^{th} elements within the thermal chimney [K], m is the mass flow rate of the air [kg/s], $C_{p,a}$ is the specific heat capacity of the air [Jkg^{-1}K^{-1}], Δx is the element length [m], and w is the width of the thermal chimney [m].

The convective heat transfer coefficient (h_c) is an empirical equation determined by Palyvos (2008) as shown in Equation 10. Palyvos had collected and tabulated solar collector convective heat transfer coefficients from various studies and developed an averaged correlation.

$$h_c = 7.4 + 4V \tag{10}$$

Where: h_c is the heat transfer coefficient [W/m^{2}K]; V is the velocity of the air [m/s].

The temperatures of the absorber and glazing walls are assumed to be uniform along the length of the chimney given the higher rate of conductive and radiative heat transfer versus convective heat transfer. Determining the convective heat transfer for the glazed wall is difficult. The surface heat transfer coefficient on the exterior side of the glass panel would vary due to changes in wind pressure coefficients alongside the face of the building from varying wind direction. As such, a conservative assumption was made for the purposes of this feasibility assessment: the glass does not transfer heat. This would underestimate the flow generated by the thermal chimney.

The radiation emitted by the absorber wall to the air is assumed to be half of the radiation transmitted through the glass. Insulation installed behind the absorber wall would increase the proportion of radiation re-emitted to the air column but a conservative assumption was made for the purposes of this assessment. It is also assumed that the negative suction forces generated by the outdoor winds at the outlet of the solar chimney would have no synergistic benefits. Air flow through the chimney is driven solely by the buoyant forces. At steady state, the maximum temperature gain of the absorber wall is limited by the rate of energy loss to the air column. The rate of energy loss cannot be greater than the rate of energy gain. This is equal to the incoming rate of radiation to the absorber wall [W/m^2] divided by the heat transfer coefficient [W/m^{2}K] to the air column. This calculated temperature gain should not exceed the sensible temperature gains assuming no

losses. This is calculated as the incoming radiation [Wh/m^2] divided by the heat capacity of the absorber wall [Wh/m^{2}k]. It was assumed that the rate of energy gain [W/m^2] is equal to the hourly energy gains in the TMY2 file [Wh/m^2] divided by the hourly period. The iterative process using Equations 8, 9 and 10 were performed until a convergence criterion of 0.01 m/s (0.03 ft/s) was met for the air velocity as changes this minimal resulted in no significant changes in the thermal comfort models. The inlet velocity generated through the iterative procedure was used to calculate the thermal comfort improvements of the suite using the various thermal comfort indicators.

Combined System Calculations

The resulting outlet velocities generated by the wind catcher and the inlet velocities required by the solar chimney were used in conjunction to determine the effects of a combined system within the suite. When both systems are operational, a conservative assumption of the suite-level air movement to be equal to the larger of the two systems is used as opposed to a hybrid mix of both. Given the complex nature of air flow, the behavior of the air through the system under varying exterior wind speeds and irradiance is unknown through spreadsheet calculations. Further ongoing research using CFD will be used to verify and compare with the assumptions made. A summary of all modeled scenarios and their descriptions are listed in Table 5.

Table 5: Summary of all modeled scenarios

Scenario	*Wind Catcher*	*Solar Chimney*	*Description*
Baseline			No passive cooling solution.
W10	✓		Wind catcher only; sized to capture 10% of the outdoor wind speed for the suite-level outlets.
W30	✓		Wind catcher only; sized to capture 30% of the outdoor wind speed at the suite-level outlet.
W50	✓		Wind catcher only; sized to capture 50% of the outdoor wind speed at the suite-level outlet.
S		✓	Solar chimney only
C10	✓	✓	Solar chimney and wind catcher sized to capture 10% of the outdoor wind speed for the suite-level outlets.
C30	✓	✓	Solar chimney and wind catcher sized to capture 30% of the outdoor wind speed for the suite-level outlets.
C50	✓	✓	Solar chimney and wind catcher sized to capture 50% of the outdoor wind speed for the suite-level outlets.

Thermal Comfort Calculations

Calculation of the PMV for the high air speeds generated by the wind catcher and solar chimney requires the use of the Standard Effective Temperature (SET) in place of air temperature as stated in ASHRAE Standard 55 Section 5.3.3. The code described in Normative Appendix B and the Informative Appendix G1 in ASHRAE Standard 55 as well as the open source code for the CBE Thermal Comfort Tool were used to determine the PMV values and SET calculations. The code was adapted for Visual Basic for Applications within Microsoft Excel and verified with the CBE Thermal Comfort Tool and the validation Table G1-1.

RESULTS AND DISCUSSION

The baseline annual PPD and cPPD is shown in Figure 3 and PMV and cPMV values are shown in Figure 4.

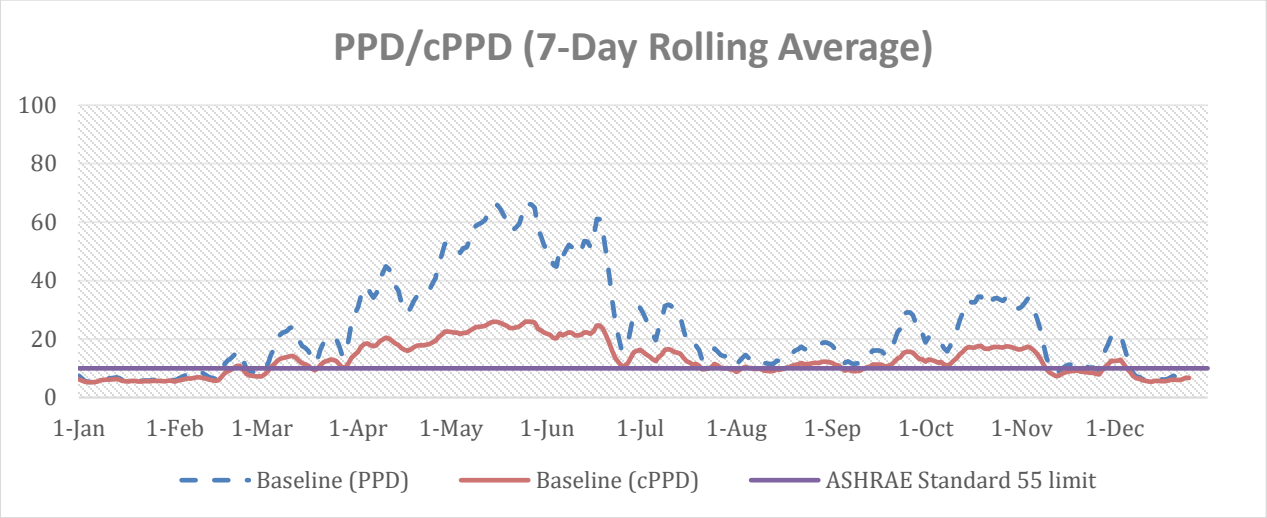

Figure 3: Baseline 7-day rolling average PPD/cPPD values

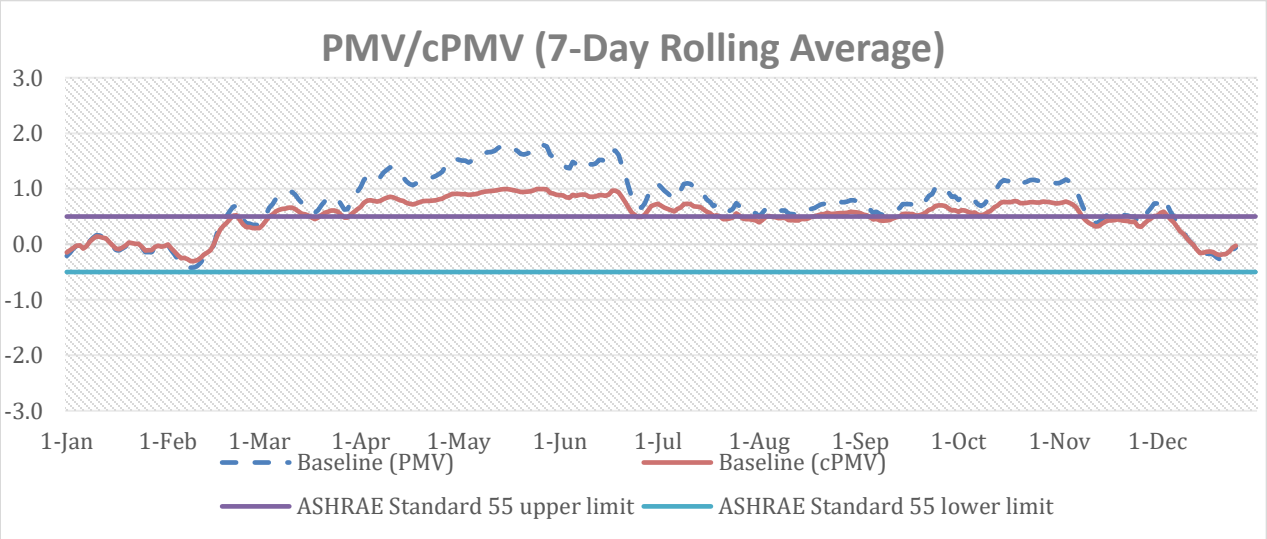

Figure 4: Baseline 7-day rolling average PPD/cPPD values

Per the PPD and PMV values calculated using ASHRAE Standard 55, exposure to the baseline conditions (as defined in "Baseline Thermal Comfort Level") would result in thermal discomfort for most the year (76%). The percentage of people dissatisfied with their environment using the ASHRAE model is greater in comparison to the cPPD and cPMV values which consider local, cultural and climatic adaptations. The cPPD and cPMV values also indicate less thermal discomfort time above limits but the proportion of time where the limits are exceeded is still high (59%). The TSI model, shown in Figure 5, has the least amount of time above comfort limits (21%) with the predicted percentage of dissatisfied being less than PPD and cPPD.

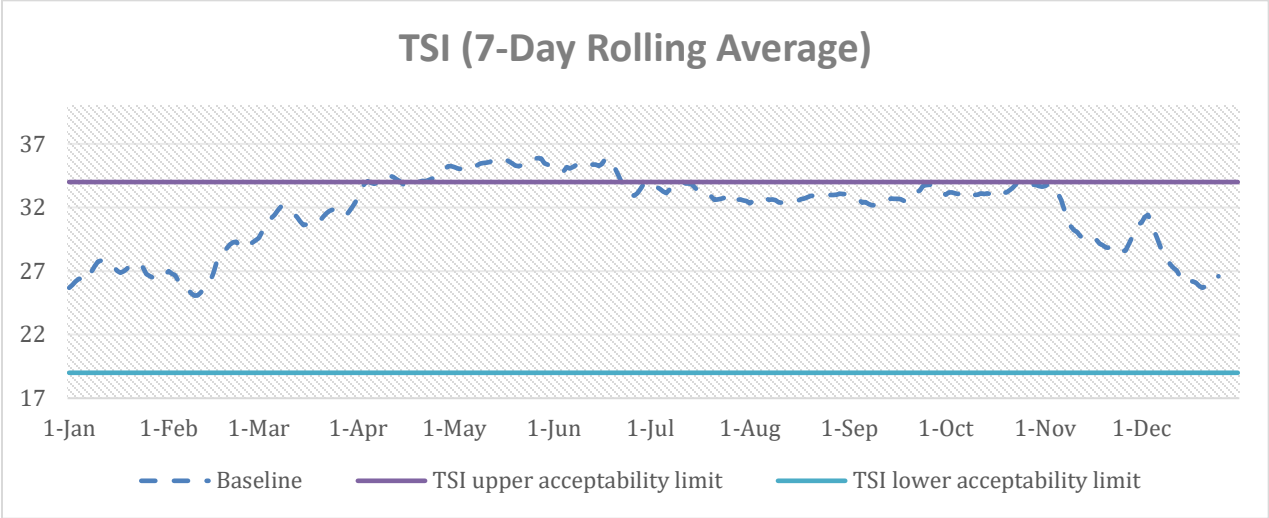

Figure 5: Baseline 7-day rolling average TSI values

Figure 6 summarizes the annual, 7-day rolling average outlet velocities generated by a W30 wind catcher and the inlet velocities generated by the solar chimney (Scenario S). The average daily velocity of the solar chimney is typically lower than the average wind velocity of W50 as the solar chimney only generates flow during daylight but is averaged over a period of twenty-four hours. In comparison to W30, the solar chimney can generate higher average velocities during periods of low seasonal winds but is lower overall during the monsoon season with its high wind speeds. During optimum conditions, the solar chimney could generate velocities up to 3.65 m/s at the inlet. Correlating with the wind rose data, wind catcher outlet velocities were highest during the monsoon season. However, the seasonal temperatures drop slightly during periods of peak wind speeds in mid-July. As thermal comfort is a function of the air movement, temperature and relative humidity, it is difficult to determine the improvements in thermal comfort without the use of thermal comfort indicators when the various parameters are changing throughout the year. By analyzing the data using the various thermal comfort indicators, a better indication of the effects of the fluctuating environmental conditions on the passive cooling system and its corresponding impact on occupant thermal comfort can be examined.

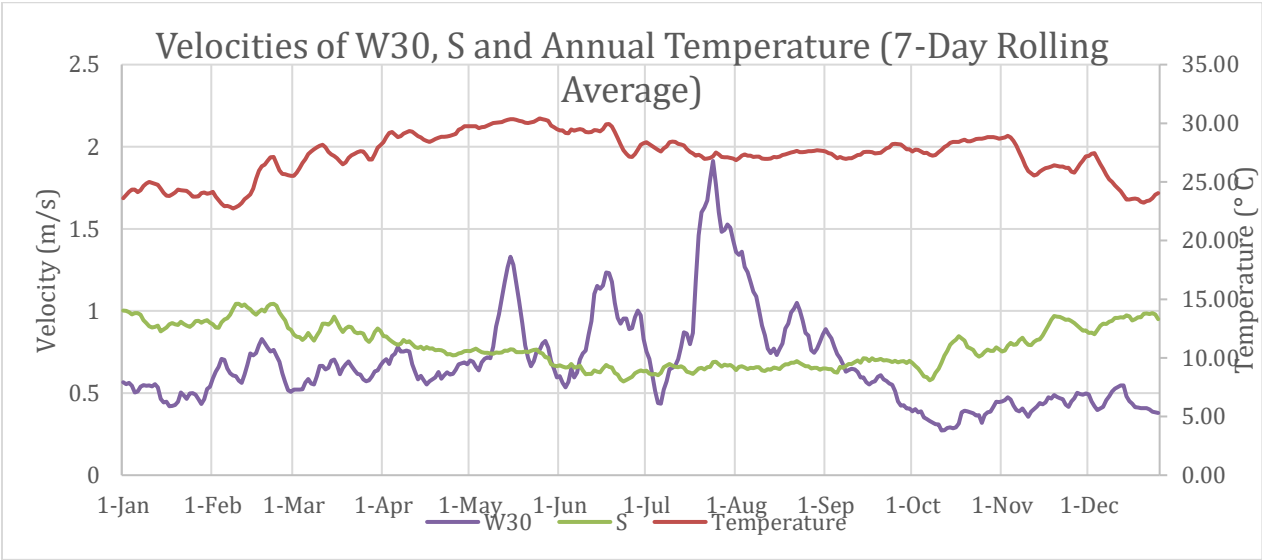

Figure 6: Average 7-day velocities generated by W30, W50 and S alongside the daily average temperature

Wind Catcher Only Scenario

Figure 7 shows the effect of the various wind catcher scenarios on the PPD throughout the year. There is a significant decrease in PPD with the addition of a wind catcher when compared to the base case. Occupants would benefit most from the solution during the monsoon and post monsoon seasons when discomfort levels are at their peaks. The time spent above ASHRAE Standard 55 limits between August and September for the base case is eliminated in Scenario W10. Overall, the annual discomfort time above Standard 55 limits decreases by 44%, 81%, and 97% relative to the baseline for Scenario W10, W30 and W50, respectively. Increasing the dimensions of the wind catcher to further decrease the hourly PPD has diminishing marginal benefits; a 37% increase in acceptability time is achieved with a 23% increase in duct area for Scenario W30 versus a 53% increase with a 108% increase in area for Scenario W50 when compared to Scenario W10. Furthermore, the differences in PPD between Scenario W30 and Scenario W50 is minimal throughout the year except during the pre-monsoon season. As such, the arguments to implement Scenario W50 over Scenario W30 is not compelling.

Figure 8 shows the effect of the various wind catcher scenarios on the cPPD throughout the year. As expected from the baseline comparisons, the cPPD values are lower in comparison to the PPD values. The predicted percentage of dissatisfied is no greater than 20% when using Singh's model in comparison to the 40% in ASHRAE for Scenario W10. Using the cPMV model, the annual discomfort time above Standard 55 limits decreases by 46%, 97%, and 100% for Scenario W10, W30 and W50 respectively.

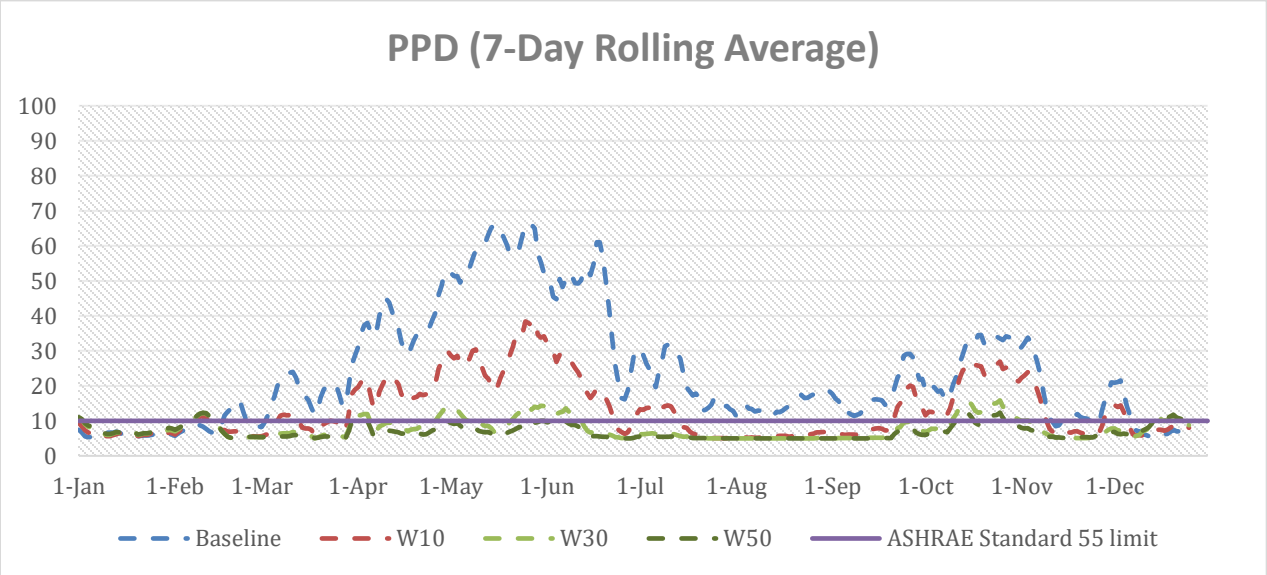

Figure 7: 7-Day rolling average PPD values for the baseline and Scenario W10, W30 and W50

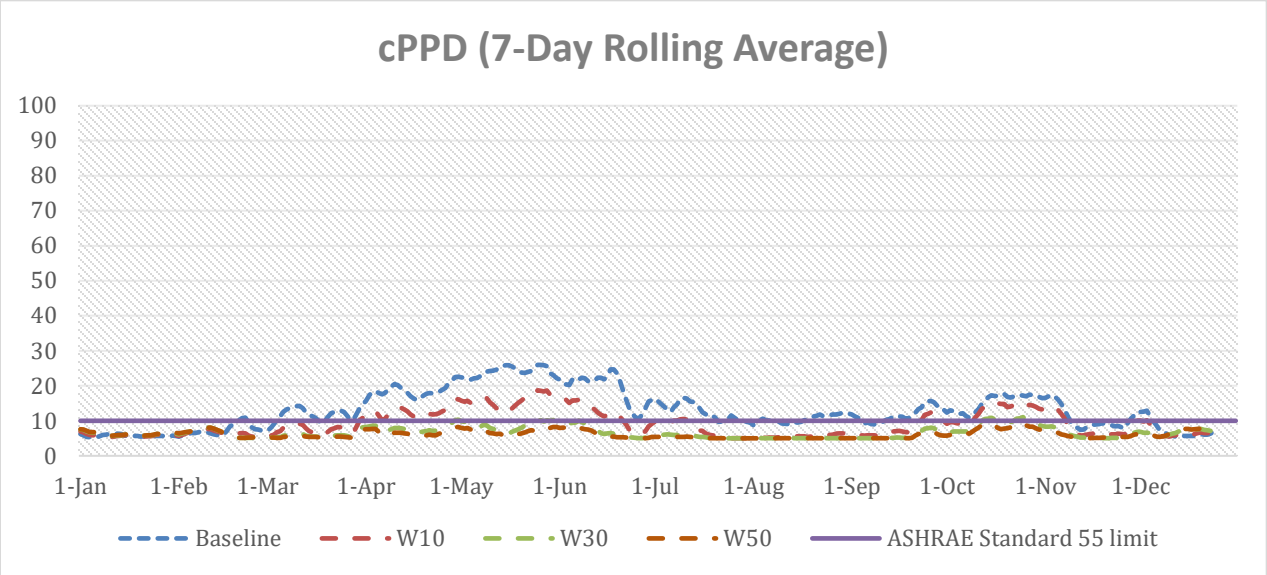

Figure 8: 7-Day rolling average cPPD values for the baseline and Scenario W10, W30 and W50

The average PPD during the winter months between late-December and mid-February increase for all scenarios. The winter seasons contain days in which both PMV values below and above the Standard 55 limits occur. As the proposed solution specifically targets discomfort due to warmth, the averaged PMV values during winter decrease below zero causing increased PPD values. This is depicted in Figure 9 which illustrates the annual 7-day rolling average PMV values.

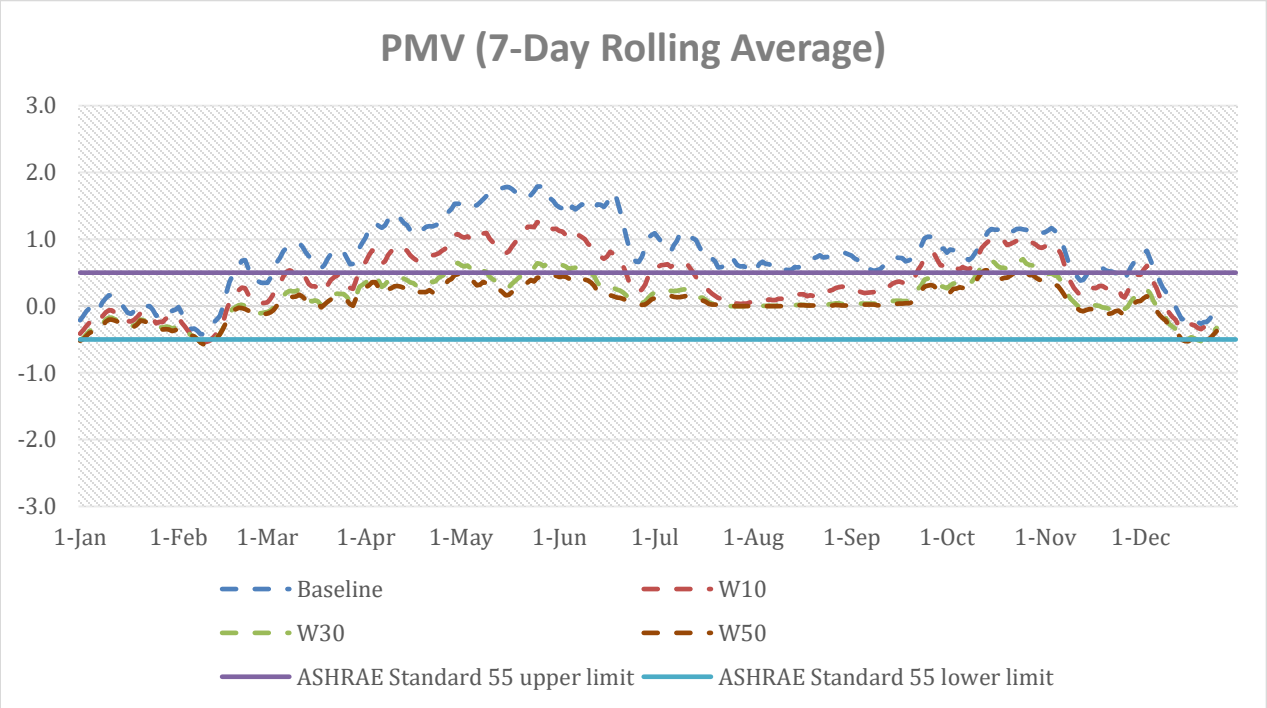

Figure 9: 7-Day rolling average PMV values for the baseline and Scenario W10, W30 and W50.

Solar Chimney and Combined Scenario

Figure 10 shows the PPD/cPPD values in different scenarios between April and August: solar chimney only (Scenario S), solar chimney plus wind catcher with 10% inlet velocity at outlet (Scenario C10), and solar chimney plus wind catcher with 30% inlet velocity at outlet (Scenario C30). The improvement in thermal comfort exclusively from the solar chimney outperforms that of Scenario W10 but not that of Scenario W30. Scenario S decreases time exceeding ASHRAE Standard 55 limits by 78% in comparison to the baseline versus the 44% and 81% for Scenario W10 and Scenario W30. Scenario C10 and Scenario C30 are shown to have lower predicted percentage of dissatisfied when compared to Scenario S and Scenario W10 while also having less time spent above limits. Table 6 summarizes the various scenarios and their reductions in discomfort time when compared to baseline levels.

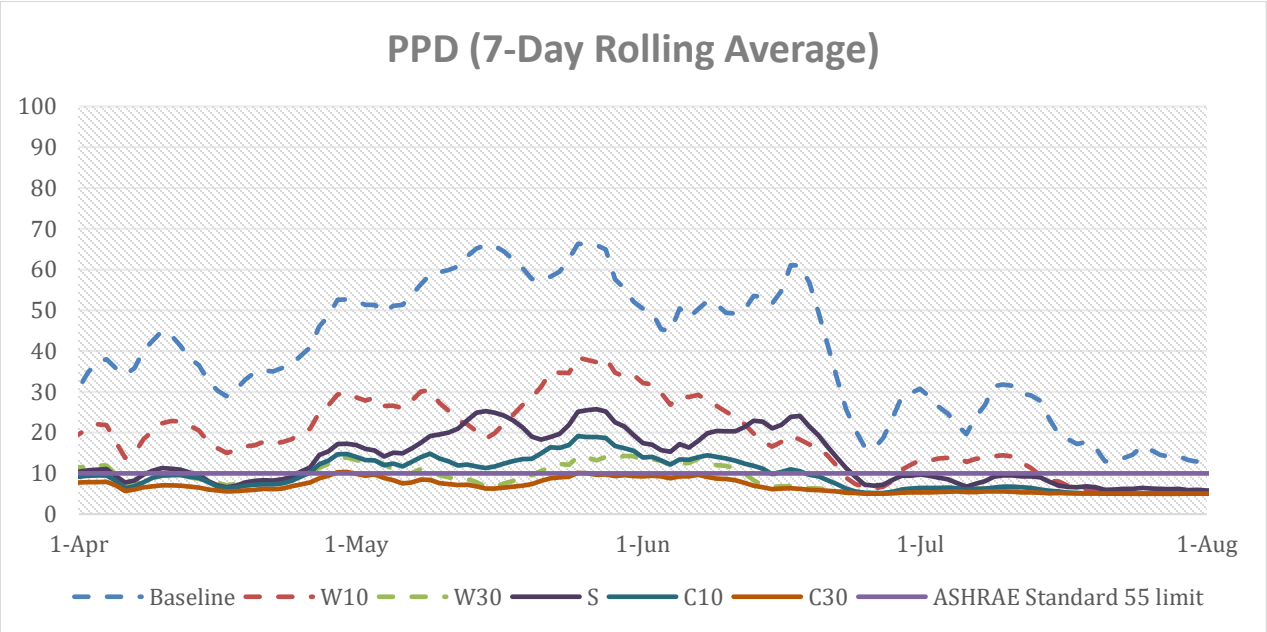

Figure 10: 7-Day rolling average PPD values for the baseline and Scenario W10, W30, S, C10 and C30.

Table 6: Summary of the total reduction in annual discomfort time compared to baseline for each scenario.

Total Reduction in Annual Discomfort Time from Baseline (%)

Scenario	W10	W30	W50	S	C10	C30	C50
Model							
PMV	44	81	97	78	81	100	100
cPMV	46	97	100	76	93	100	100
TSI	11	23	28	23	24	26	31

CONCLUSION

The effects of a wind catcher and solar chimney on thermal comfort in MURBs was examined. The unaffordability of cooling technologies for those in lower income brackets and the projected energy demands in India provide a unique opportunity for the application of passive cooling strategies to mitigate their energy consumption and reach their carbon reduction goals. The literature indicates that wind catchers and solar chimneys could help solve the gap. The expected range of velocities at the outlet of the wind catcher were determined using fundamental equations. Calculations, based on the TMY2 weather data files provided by ISHRAE, were performed to determine the effects on thermal comfort through various wind catcher and solar

chimney configurations. The wind catchers which could output 30% of the inlet velocity (Scenario W30) was shown to decrease the total annual discomfort time above limits by 97% and 81% when using the cPMV and PMV respectively. Solar chimneys were less effective in decreasing the overall time above limits when compared to Scenario W30 but performed better than Scenario W10. Overall, the combination of both approaches has better reliability in decreasing discomfort time above the respective limits of each model (a minimum reduction of 81%). Further research would be required to verify the effects of the wind catcher and solar chimney on the MURB but these initial results show promise. The CFD testing to follow will allow for a more complete analysis of the synergistic effects of the exterior wind on the solar chimney and the interactions between the solar chimney and the wind catcher with regards to the suite-level air movement. This optimization will include orientation of the solar chimney, design of the chimney absorber wall, as well as the wind catcher duct dimensions and inlet design. The streamlines within the suite generated by the wind catcher and the solar chimney will be further investigated and modeled with CFD to determine the air velocities experienced by the occupants in the suites.

REFERENCES

Amori, K.E., and Mohammed, S.W. 2012. Experimental and numerical studies of solar chimney for natural ventilation in Iraq. Energy and Buildings, 47: 450–457. doi:10.1016/j.enbuild.2011.12.014.

Asadi, S., Fakhari, M., Fayaz, R., and Mahdaviparsa, A. 2016. The effect of solar chimney layout on ventilation rate in buildings. Energy and Buildings, 123: 71–78. doi:10.1016/j.enbuild.2016.04.047.

ASHRAE. 2013. Thermal Environmental Conditions for Human Occupancy. Ashrae, ASHRAE Sta: 58.

Aynsley, R.M., Melbourne, W.H., and Vickery, B.J. 1977. Architectural Aerodynamics. Applied Science Publishers, 1977.

Bansal, N.K., Mathur, R., and Bhandari, M.S. 1993. Solar chimney for enhanced stack ventilation. Building and Environment, 28(3): 373–377. doi:10.1016/0360-1323(93)90042-2.

Bijli Bachao Team. 2017. Domestic Electricity LT Tariff Slabs and Rates for all states in India in 2016 : Bijli Bachao. Available from https://www.bijlibachao.com/news/domestic-electricity-lt-tariff-slabs-and-rates-for-all-states-in-india-in-2016.html [accessed 13 February 2017].

Carrilho da Graça, G., Chen, Q., Glicksman, L.R., and Norford, L.K. 2002. Simulation of wind-driven ventilative cooling systems for an apartment building in Beijing and Shanghai. Energy and Buildings, 34(1): 1–11. doi:10.1016/S0378-7788(01)00083-4.

Fatimah, W., Yusoff, M., Sapian, A.R., Salleh, E., Adam, M., and Johar, S. (n.d.). I Indoor ndoor and and Built uilt Environment Application of solar-induced ventilation prototype in small and medium enterprise building. doi:10.1177/1420326X13512143.

Gallo, C. 1996. Passive cooling as design methodology: some examples from the past to the present. Renewable Energy, 8(1–5): 309–314.

India Meteorological Department. (n.d.). Frequently Asked Questions.

Indraganti, M. 2010a. Adaptive use of natural ventilation for thermal comfort in Indian apartments. Building and Environment, 45(6): 1490–1507. doi:10.1016/j.buildenv.2009.12.013.

Indraganti, M. 2010b. Behavioural adaptation and the use of environmental controls in summer for thermal comfort in apartments in India. Energy and Buildings, 42(7): 1019–1025. doi:10.1016/j.enbuild.2010.01.014.

ISHRAE. 2005. Indian Weather Data from the Indian Society of Heating, Refrigerating and Air-Conditioning Engineers. New Delhi, India.

Lee, K.H., and Strand, R.K. 2009. Enhancement of natural ventilation in buildings using a thermal chimney. Energy and Buildings, 41(6): 615–621. doi:10.1016/j.enbuild.2008.12.006.

Li, J., and Li, D. 2015. The Study on Numerical Simulation of Classrooms Using Hybrid Ventilation Under Different Solar Chimney Radiation. Procedia Engineering, 121: 1083–1088. doi:10.1016/j.proeng.2015.09.105.

Mavrogianni, A., and Mumovic, D. 2009. On the Use of Windcatchers in Schools: Climate Change, Occupancy Patterns, and Adaptation Strategies. Indoor and Built Environment, 19(3): 340–354. doi:10.1177/1420326X09341507.

Ministry of New and Renewable Energy. (n.d.). INDIA SOLAR RESOURCE MAPs. Available from http://mnre.gov.in/sec/solar-assmnt.htm [accessed 1 June 2017].

Nouaneue, H.F., Alandji, L.R., and Bilgen, E. 2008. Numerical study of solar-wind tower systems for ventilation of dwellings. Renewable Energy, 33: 434–443. doi:10.1016/j.renene.2007.03.001.

Palyvos, J.A. 2008. A survey of wind convection coefficient correlations for building envelope energy systems' modeling. Applied Thermal Engineering, 28(8–9): 801–808. doi:10.1016/j.applthermaleng.2007.12.005.

Priyadarsini, R., Cheong, K.W., and Wong, N.H. 2004. Enhancement of natural ventilation in high-rise residential buildings using stack system. Energy and Buildings, 36(1): 61–71. doi:10.1016/S0378-7788(03)00076-8.

Sauer, H.J., Howell, R.H., and Coad, W.J. 2013. Principles of Heating Ventilating and Air Conditioning: A Textbook with Design Data Based on the 2013 ASHRAE Handbook Fundamentals.

Singh, M.K., Mahapatra, S., and Atreya, S.K. 2011. Adaptive thermal comfort model for different climatic zones of North-East India. Applied Energy, 88(7): 2420–2428. doi:10.1016/j.apenergy.2011.01.019.

Society for Participatory Research in Asia. 2014. Contributions of the Urban Poor and Challenges for Urban Governance in Chhattisgarh. Available from http://www.pria.org/event-details-contributions-of-the-urban-poor-and-challenges-for-urban-governance-in-chhattisgarh-26-174 [accessed 12 February 2017].

Su, Y., Lei, F., and Xue, Y. (n.d.). Modeling of natural ventilation in solar chimney and optimization of the channel profile by CFD method. doi:10.4028/www.scientific.net/AMM.368-370.549.

The World Bank. 2008. Residential Consumption Of Electricity In India Background paper India: Strategies

for Low Carbon Growth Draft. The World Bank, (July): 1–73. doi:http://www.moef.nic.in/downloads/public-information/Residentialpowerconsumption.pdf.

The World Bank. 2016. Intended Nationally Determined Contributions (INDCs). Available from http://spappssecext.worldbank.org/sites/indc/Pages/INDCHome.aspx.

Udaykumar, A., Rajasekar, E., and Venkateswaran, R. 2013. Thermal comfort characteristics in naturally ventilated, residential apartments in a hot-dry climate of India. Indoor and Built Environment, 24(1): 101–115. doi:10.1177/1420326X13504120.

Wilson, D.J. 1979. Flow Patterns Over Flat-Roofed Buildings and Application To Exhaust Stack Design. ASHRAE Transactions, 85(Pt 2): 284–295.

Zamora, B., and Kaiser, A.S. 2010. Numerical study on mixed buoyancy-wind driving induced flow in a solar chimney for building ventilation. Renewable Energy, 35: 2080–2088. doi:10.1016/j.renene.2010.02.009.